Applied Catalysis A: General 404 (2011) 141–148

Contents lists available at ScienceDirect

Applied Catalysis A: General

journal homepage: www.elsevier.com/locate/apcata

Catalytic conversion of alcohols over alumina–zirconia mixed oxides: Reactivity and selectivity

Hossein A. Dabbagh*, Mehdi Zamani

Catalysis Research Laboratory, Department of Chemistry, Isfahan University of Technology, Isfahan, Iran

ARTICLE INFO

Article history:
Received 5 May 2011
Received in revised form 14 July 2011
Accepted 16 July 2011
Available online 22 July 2011

Keywords:
Amorphous
Crystalline
Mixed Al_2O_3–ZrO_2
Catalyst reactivity-selectivity
Dehydration

ABSTRACT

The amorphous and crystalline mixed 25, 50 and 75 wt.% Al_2O_3–ZrO_2 composites were prepared by means of sol–gel method using aluminum iso-propoxide and zirconyl nitrate precursors. Physicochemical properties were determined using XRD, BET, NH_3-TPD, TGA, SEM, and FT-IR spectroscopy. Catalytic activity and selectivity were investigated for the dehydration of 2-octanol and 1,2-diphenyl-2-propanol (DPP). $Al_{75}Zr_{25}$ composite is more selective than other forms for the conversion of 2-octanol. The selectivity of DPP for 1-alkene formation was increased over $Al_{25}Zr_{75}$ catalyst. The crystalline 50 wt.% catalyst dehydrated tertiary alcohol (DPP) selectively in the presence of 2-octanol. The amorphous 50 wt.% catalyst dehydrated DPP predominately to 1-alkene isomer. The crystalline catalyst favored the formation of *E*-2-alkene.

1. Introduction

Alumina and zirconia are widely used in many important technological applications [1–6]. Zirconia exhibits various structural polymorphs including cubic (c-ZrO_2), tetragonal (t-ZrO_2) and monoclinic (m-ZrO_2) structures which are formed below the melting point (2680 °C), below 2370 °C and below 950 °C, respectively [7]. Addition of appropriate dopants, such as Ca^{2+}, Mg^{2+}, or Y^{3+} is known to stabilize the tetragonal and cubic polymorphs [8–11].

$$\text{Liquid} \xrightarrow{\approx 2680^\circ C} \text{c-}ZrO_2 \xrightarrow{\approx 2370^\circ C} \text{t-}ZrO_2 \xrightarrow{\approx 950-1150^\circ C} \text{m-}ZrO_2$$

Alumina also exhibits a remarkable series of structural polymorphs including α-Al_2O_3 and a large variety of metastable forms. The metastable variants are a series of transition aluminas, which form by dehydration of aluminum hydroxides and oxyhydroxides [12].

$$\gamma\text{-AlOOH} \xrightarrow{\approx 500^\circ C} \gamma\text{-}Al_2O_3 \xrightarrow{\approx 850^\circ C} \delta\text{-}A_2O_3 \xrightarrow{\approx 1000^\circ C} \theta\text{-}Al_2O_3 \xrightarrow{\geq 1100^\circ C} \alpha\text{-}Al_2O_3$$

Depending on the method and preparation conditions, different phases are generated in mixed Al_2O_3/ZrO_2 oxides [13–19]. Sarkar et al. [13] used the aluminum nitrate and zirconyl chloride precursors to prepare alumina/zirconia (5–10 wt.% ZrO_2) composites. They reported that the catalysts calcined at 200 °C were boehmite (AlOOH) and bayerite ($Al(OH)_3$). At 1400 °C the t-, m-zirconia and α-alumina were crystallized. Zawadzki et al. [14] used aluminum iso-propoxide and zirconyl nitrate to prepare 10 wt.% ZrO_2 composites. They reported that boehmite crystallized to γ-alumina at 600 °C while, t-zirconia and α-alumina crystallized at 1200 °C. Kagawa et al. [15] reported that by increasing of Al_2O_3 content in the mixed oxide, the amount of the m-ZrO_2 decreased, thus indicating the stabilization of the t-ZrO_2 by the Al_2O_3.

Preparation of amorphous Al_2O_3–ZrO_2 materials was reported using sol–gel method [16–19], laser-splatting [16], plasma spraying [16], electrohydrodynamic atomization [17] and melt extraction [18]. Soisuwan et al. [19] prepared alumina–zirconia mixed oxides with 0.5, 1, 25, 40, and 75 mol% of alumina in zirconia using aluminum nitrate and zirconyl chloride precursors. In composites calcined at 600 °C with low Al contents (<25%), tetragonal phase zirconia was observed, while at higher Al contents, the mixed oxide exhibited only the amorphous phase. Han et al. [20,21] used the aluminum iso-propoxide and zirconium butoxide to prepare amorphous mixed 50 wt.% alumina/zirconia composite. The calcined composites powders were amorphous at 400 °C. By increasing the calcination temperature to 980 and 1200 °C, the c- and t-ZrO_2 were crystallized, respectively. Beitollahi et al. [22] reported the preparation of amorphous mixed Al_2O_3–ZrO_2 using aluminum nitrate and zirconyl chloride at 500 °C calcination temperature. At higher temperatures the various alumina metastable phases were formed. Most of these works were restricted to the synthesis and morphology of composites. A detailed understanding of

* Corresponding author. Tel.: +98 311 391 3257; fax: +98 311 391 2350.
E-mail address: dabbagh@cc.iut.ac.ir (H.A. Dabbagh).

0926-860X/$ – see front matter © 2011 Elsevier B.V. All rights reserved.
doi:10.1016/j.apcata.2011.07.024

their catalytic activity for dehydration reaction of alcohols is still lacking.

Recently, selectivity and reactivity of alcohols over pure alumina and mixed alumina–thoria was investigated by Dabbagh et al. [23–25]. We reported a decrease in the reactivity but no change in the selectivity in the dehydration of secondary and tertiary alcohols by mixed γ-alumina–thoria [24]. In this work chemically mixed amorphous Al_2O_3–ZrO_2 powder (25, 50 and 75 wt.%) were synthesized using the sol–gel method with aluminum iso-propoxide and zirconyl nitrate. Characterization of the catalysts was performed by X-ray diffraction (XRD), thermo gravimetric analysis (TGA), scanning electron microscopy (SEM) and infrared spectroscopy (IR). Evaluation of catalytic activity and selectivity was investigated for dehydration of 2-octanol and DPP were monitored by gas chromatography (GC) and gas chromatography mass spectrometry (GC–MS) techniques.

2. Experimental

2.1. Catalyst preparation

Aluminum iso-propoxide [$Al(OC_3H_7)_3$] and zirconyl nitrate [$ZrO(NO_3)_2{\cdot}xH_2O$] were purchased from Aldrich. Five samples of chemically mixed oxides were prepared with different composition of aluminum iso-propoxide:zirconyl nitrate wt.% (100:0, 75:25, 50:50, 25:75 and 0:100) using the sol–gel method. The samples are called $Al_{100}Zr_0$, $Al_{75}Zr_{25}$, $Al_{50}Zr_{50}$, $Al_{25}Zr_{75}$ and Al_0Zr_{100}, respectively. Initially, aluminum iso-propoxide and zirconyl nitrate with different composition (100:0, 75:25, 50:50, 25:75 and 0:100 wt.%) were mixed well. Then excess amount of water (precursor/water wt.% ratio = 2 for $Al_{100}Zr_0$ and 4 for $Al_{75}Zr_{25}$, $Al_{50}Zr_{50}$, $Al_{25}Zr_{75}$ and Al_0Zr_{100}) was added to this mixture with continuous stirring for 1 h at room temperature. Finally the gel solution was heated for 24 h at 120 °C to remove the solvent and to allow maximum interaction of the metal hydroxides. The dried gel was calcined at 600 or 1000 °C (heating rate of 2 and 5 °C/min, respectively) and remained at these temperatures for 6 h under air atmosphere. The mechanically mixed $Al_{50}Zr_{50}$ composite was prepared by physically mixing and milling of the equal ratios of alumina and zirconia ($Al_{100}Zr_0$ (50%) and Al_0Zr_{100} (50%)) samples. This mixture was prepared to indicate the physical mixing and should not be compared to the chemically mixed $Al_{50}Zr_{50}$ from iso-propoxide and zirconyl nitrate weight ratios.

2.2. Characterization of catalysts

The X-ray diffraction patterns were recorded by employing a Philips Xpert MPD diffractometer using Cu Kα radiation (λ = 1.54 Å) in the range of 20–90° (2θ) with a step size of 0.03° (2θ) and a counting time of 16 s for the samples. The Brunauer–Emmett–Teller (BET) specific surface areas were measured at the boiling point of nitrogen (196 °C) after outgassing at 300 °C using an ASAP 2000. The NH_3-TPD of the calcined catalysts was assessed through thermal programmed adsorption/desorption of NH_3 in a quartz reactor by rising the temperature (10 °C/min heating rate) from 100 to 800 °C using frontal chromatography technique through Micromeritics TPD-TPR 2900 system. The TPD of 200 mg for each sample was performed under helium (gas rate: 40 Ncc/min). Scanning electron microscopy was performed by Philips XCL microscope. Gold is vapor-deposited over samples before analysis. The thermal decomposition behavior of the dried gel was studied by TG–DTA analysis (Linseis, L70/2171 model) up to 1200 °C with heating rate of 10 °C/min under atmospheric pressure. The infrared spectra were obtained using a Jasco-FT-IR-680 plus spectrometer in the wave number range 400–4000 cm^{-1}. Catalysts were diluted in KBr with the ratio of 1:100 (catalysts: KBr).

2.3. Dehydration reaction

The conversion of alcohols was performed in a vertical plug flow reactor made of Pyrex glass and fitted with a thermal well that extended to the center of the catalyst bed. The Pyrex glass beads (20–30 cm^3 of the reactor volume above the catalyst bed) were used to serve as pre-heater. Adducts were collected (with increasing time intervals) at room temperature. The conversion of 2-octanol (98 wt.%) and DPP (2 wt.%) mixture at 280 °C (reaction temperature) with flow rate of 18 cm^3/h over 2.0 g of catalyst was monitored by Agilent 6890N gas chromatography using 30 m × 0.32 mm HP-5 column packed with (5% phenyl)-methylpolysiloxane. DPP is solid which was prepared according to the Grignard method reported earlier [23]. 2-Octanol and DPP were selected for the following reasons. First, the dehydration of secondary and tertiary alcohols was investigated in one run under identical conditions. The amounts of catalyst, reaction temperature, mesh size and flow rate were kept constant. Second, high concentration of 2-octanol was used as solvent to prevent isomerization. Analysis of the product mixture was carried out by gas chromatography mass spectrometry Fisons 8060 instrument (QD analyzer and Trio 1000 detector model) equipped with a 30 m HP-5 capillary column.

3. Results and discussion

3.1. Catalysts characterization

Recently, dehydration of aluminum hydroxide to form pure γ-alumina was reported as a polymerization process. The monomer aluminum hydroxide undergoes polymerization by losing water molecules with random cross-linkage (in three dimensions) between the polymer chains [23,24]. The rate of dehydration of this precursor is too fast and difficult to control. Initially, the boehmite precipitates and peptidizes to a sol. A transparent gel was obtained by evaporating the solvent from the sol. The number of cross-linkages was increased (by loss of more water molecules) and the number of vacancies decreased leading to a very low surface area of α-alumina (a complete cross-linked polymer) at higher temperatures (from 200 to 1200 °C). The side product of the hydrolysis of $Al(OC_3H_7)_3$ is isopropyl alcohol (Eq. (1)). The main advantage of this precursor is that it does not require any additives. The co-polymerization process was catalyzed by HNO_3 during the hydrolysis of $ZrO(NO_3)_2{\cdot}xH_2O$ (Eq. (2)). The amorphous phase was produced by random cross-linkages during the hydrolysis of the precursor at 200–600 °C. A crystalline phase was produced at higher temperatures (above 900 °C). Fig. 1 shows the photograph of mixed oxide gels dried at 120 °C. The color of $Al_{75}Zr_{25}$ composite was orange, while the $Al_{50}Zr_{50}$ and $Al_{25}Zr_{75}$ composites were yellow and creamy, respectively. The color of composites was related to amounts of nitrous and nitrate compounds formed during reaction between isopropyl alcohol and HNO_3 (Eq. (3)).

Fig. S1 shows SEM pictures of $Al_{75}Zr_{25}$ and $Al_{50}Zr_{50}$ composites dried at 120 °C. The large rod (Fig. S1e,g), needle (Fig. S1h) and bulk (Fig. S1e) shapes were observed for $Al_{50}Zr_{50}$ composite. The helix (Fig. S1a,c) and bulk (Fig. S1a,b) structures were existing for $Al_{75}Zr_{25}$ composite. The bulk structures of both mixed oxides composed of small agglomerated particles (Fig. S1d,f). The length of rod shape composites was estimated about 2–3 mm with diameter larger than 120 μm. The needle shape composites have nearly 500 μm length and their diameters at the end and tip of needle are almost 6 and 50 μm, respectively. The length of helix shape

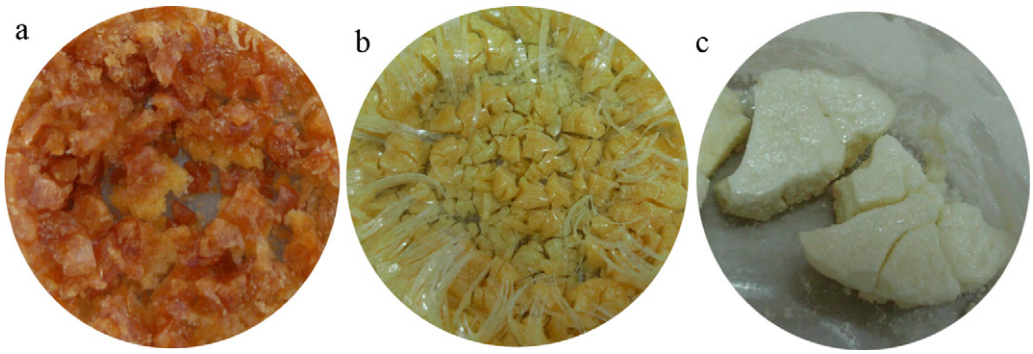

Fig. 1. Morphology of mixed Al_2O_3–ZrO_2 composites with different compositions dried at 120 °C (a) $Al_{75}Zr_{25}$, (b) $Al_{50}Zr_{50}$ and (c) $Al_{25}Zr_{75}$.

composites was estimated several millimeters with diameter larger than 60 μm.

$$Al(OCH(CH_3)_2)_3 + 2H_2O \rightarrow AlO(OH) + 3(CH_3)_2CHOH \quad (1)$$

$$ZrO(NO_3)_2 + 2H_2O \rightarrow ZrO(OH)_2 + 2HNO_3 \quad (2)$$

$$(CH_3)_2CHOH + 2HNO_3 \rightarrow (CH_3)_2CHONO + (CH_3)_2CHONO_2 + H_2O \quad (3)$$

Fig. 2 shows the X-ray diffraction patterns of calcinated Al_2O_3–ZrO_2 mixed oxides ($Al_{100}Zr_0$, $Al_{75}Zr_{25}$, $Al_{50}Zr_{50}$, $Al_{25}Zr_{75}$, and Al_0Zr_{100} at 600 °C). The XRD pattern of the pure γ-Al_2O_3 predicts four (3 1 1), (4 0 0), (4 4 0) and (5 1 1) diffraction lines at (2θ) 39°, 46°, 67° and 85°, which were compatible with the γ-alumina spectrum reported in the literature [26]. Pure zirconia was prepared from a mixture of two monoclinic and tetragonal phases. t-ZrO_2 has four well-known diffraction lines at 2θ 30° (1 1 1), 50° (2 2 0), 60° (3 1 1) and 63° (2 2 2). The (1 1 0) and (1 1 1) diffraction lines of m-ZrO_2 appeared at 2θ 28° and 32°, respectively. The related JCPDS files are shown in the supporting information (Figs. S3–S6). The $Al_{75}Zr_{25}$, $Al_{50}Zr_{50}$, and $Al_{25}Zr_{75}$ composites are approximately amorphous and did not indicate distinct peaks in their XRD patterns. The XRD patterns of $Al_{50}Zr_{50}$ composites at various temperatures are shown in Fig. 3. In the dried gel (at 120 °C) and calcinated sample at 600 °C no XRD peaks was detected, while both tetragonal zirconia and α-alumina peaks were detected at 1000 °C. Fig. 3c shows the XRD pattern of mechanically mixed $Al_{50}Zr_{50}$ composites at 600 °C. In this sample all peaks of γ-alumina and t, m-zirconia were detected.

The XRD patterns for mixture of m, t-ZrO_2 (dashed line) and crystalline mixed Al_2O_3–ZrO_2 (50 wt.%) composite calcined at 1000 °C (solid line) is depicted in Fig. 4. The diffraction (1 1 1), (2 2 0), (3 1 1) and (2 2 2) lines of crystalline mixed Al_2O_3–ZrO_2 slightly shifted and drastically broadened from the initial positions of the pure ZrO_2. Also, by doping of ZrO_2 with alumina, the m-ZrO_2 phase was eliminated and the tetragonal phase was stabilized. This observation complements the results published by Kagawa et al. [15]. They reported that the m-ZrO_2 phase was decreased with the increase in alumina content which coincides with stabilization of the t-ZrO_2 phase.

Fig. S2 shows SEM photograph of Al_2O_3–ZrO_2 (50 wt.%) composites which was formed under different experimental conditions. The flat plane shape structures (Fig. S2a) was detected in the chemically mixed $Al_{50}Zr_{50}$ composite calcined at 600 °C, while mechanically mixed $Al_{50}Zr_{50}$ composite have porous structure (Fig. S2b). These results indicated that there are distinct differences between chemically and mechanically mixed Al_2O_3–ZrO_2 composites. The composite calcined at 1000 °C showed limacone (Fig. S2c) and agglomerated (Fig. S2d) shapes.

The specific BET surface areas for the $Al_{50}Zr_{50}$ mixed oxides calcined at 600 and 1000 °C were 104.2 and 0.3 m^2/g, respectively. The specific BET surface area for the γ-alumina prepared under the same condition was reported 150 m^2/g [23,25]. The aluminas with crystalline structure which were synthesized by different methods showed similar surface properties [27]. The zirconia solids generally have a low surface area of 20–50 m^2/g [20,28].

Figs. S7 and S8 (supporting information) show the NH_3-TPD profile for the calcined $Al_{50}Zr_{50}$ catalysts at 600 and 1000 °C,

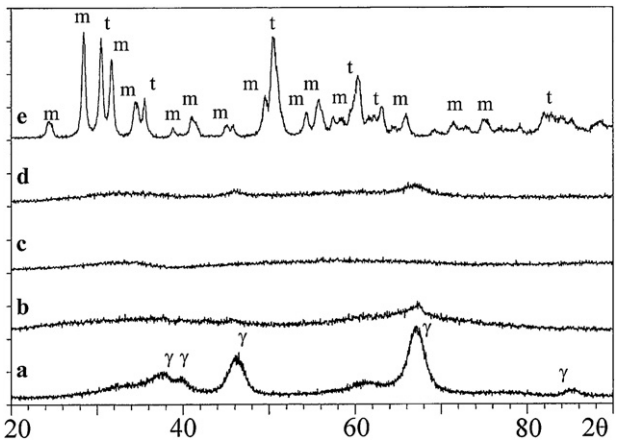

Fig. 2. XRD patterns of mixed Al_2O_3–ZrO_2 composites with different compositions calcined at 600 °C: (a) $Al_{100}Zr_0$, (b) $Al_{75}Zr_{25}$, (c) $Al_{50}Zr_{50}$, (d) $Al_{25}Zr_{75}$ and (e) Al_0Zr_{100}.

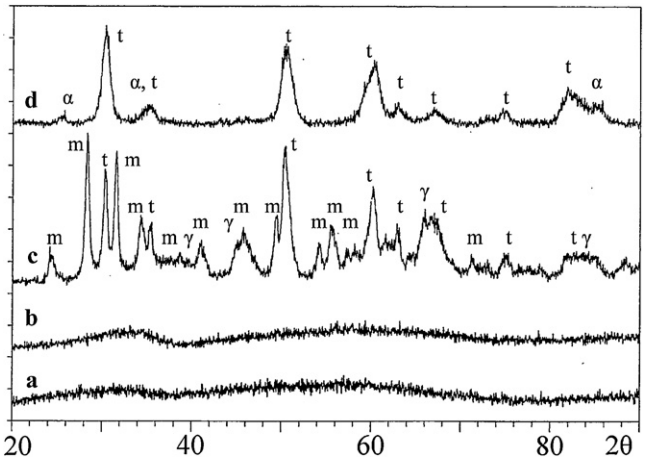

Fig. 3. XRD patterns of chemically (a, b, d) and mechanically (c) $Al_{50}Zr_{50}$ composites at deferent conditions: (a) dried at 120 °C, (b, c) calcined at 600 °C and (d) calcined at 1000 °C.

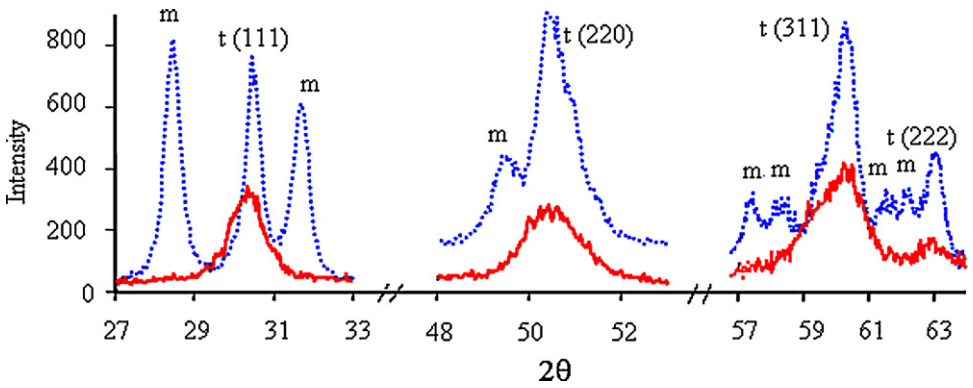

Fig. 4. Portion of the XRD patterns of pure ZrO_2 (blue dashed line, —) and crystalline mixed Al_2O_3–ZrO_2 (50 wt.%) oxides (red solid line, —) calcined at 1000 °C. (For interpretation of the references to color in this figure legend, the reader is referred to the web version of the article.)

respectively. The profile of amorphous catalyst indicates two strong peaks at 263 and 630 °C corresponding to desorbed 3.41 and 6.15 mmol NH_3/g, respectively. Crystalline catalyst did not show a significant peak at 263 °C, but a weak peak at 664 °C corresponding to desorbed 0.08 mmol NH_3/g. Unfortunately, calculation of the number of acid sites was not possible with the instrument in use. These desorbed values correspond to both acid sites and the trapped ammonia inside the bulk. The NH_3-TPD data, however, complements the BET finding.

The DTA–TG curve of $Al_{50}Zr_{50}$ composite dried gel is shown in Fig. 5. A weigh loss about 42% was observed from room temperature to about 500 °C. The initial endothermic peak at range 60–150 °C was attributed to the removal of physically and chemically adsorbed water present in the pores of the gel. The second endothermic peak at 200–320 °C corresponds to the dehydration of the aluminum hydroxides and oxyhydroxides. This temperature range encompasses important thermal processes such as transition alumina creation which starts below 300 °C [25]. Removal of

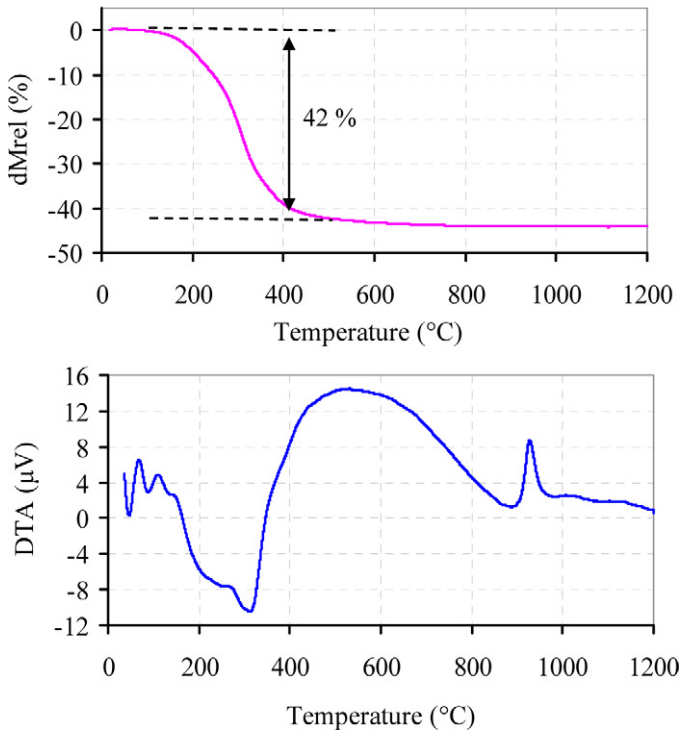

Fig. 5. TG (top) and DTA (bottom) curves of $Al_{50}Zr_{50}$ composite dried gel.

the doped nitrate ions from pores and vacancies occurred at higher temperatures (320–500 °C). The exothermic peak at around 920 °C was related to the crystallization of α-Al_2O_3 and t-ZrO_2. This feature was shown clearly by the XRD measurements (Fig. 3).

Fig. 6 shows the FT-IR spectra of the catalysts calcined at different temperatures (120, 600 and 1000 °C). The stretching Al–O vibrational modes of alumina gel dried at 120 °C are responsible for the appearance of four peaks at 475, 619, 735 and 1072 cm^{-1}. It is known that the band characterized of boehmite appear at 1072 cm^{-1}, therefore the disappearance of this peak in the sample calcinated at 600 °C indicates the formation of γ-alumina phase. The stretching OH modes of boehmite were observed at 3096 and 3420. These peaks were shifted to 3445 cm^{-1} for the calcinated samples. The bands at 420, 574 and 747 cm^{-1} were assigned to the stretching vibrations of Zr–O in monoclinic phase. The corresponding value for tetragonal phase appeared at 497 cm^{-1}. The Al–OH and Zr–OH bending vibrational modes of $Al_{75}Zr_{25}$, $Al_{50}Zr_{50}$ and $Al_{25}Zr_{75}$ catalysts were observed at 1637 (1635 or 1636 for pure alumina) and 1384 cm^{-1} (was observed for pure alumina and zirconia at lower temperatures), respectively. These results are in good agreement with the reported values for alumina [13,24,25,29–31] and zirconia [13,31,32] materials.

The FT-IR spectra of composites are different from those of pure materials. The mixed oxide gel dried at 120 and 600 °C exhibited a broad strong stretching OH vibration at 2500–3700 cm^{-1}, while the mixed oxide calcined at 1000 °C showed strong OH vibrations. In dried gel of composites (at 120 °C) the stretching nitrate peaks appeared at 1541 and 1384 cm^{-1}. The Al–O and Zr–O vibrations in the dried gel and calcined composites at 600 °C are inconclusive (because of the amorphous nature of composites with overlapped modes). The sharp signal was observed at 1000 cm^{-1} for the calcined (at 1000 °C) $Al_{50}Zr_{50}$ composites, because of the samples crystallinity. The Al–OH bending vibrations appeared at 1638 and 1385 cm^{-1} which are in agreement with Sarkar et al. work [13]. The increment of intensity at 1637 cm^{-1} and elimination of 1385 cm^{-1} mode for crystalline catalyst in comparison to amorphous composite are attributed to appearance of t-ZrO_2 phase. The amount of free OH groups on the surface of α-Al_2O_3 was reported very low [12] this complements the disappearance of 1384 cm^{-1} mode in the crystalline catalyst. Examination of the OH stretching region should be taken with caution since the use of ex situ IR with KBr pellets prevents a thorough discussion of the intensity and peak position in the OH region. Bands assigned to Al–OH and Zr–OH bending modes may well be alternatively assigned to water and nitrate ions. However, the relative comparison of the FT-IR spectra shed some light to the complex structure of these oxides.

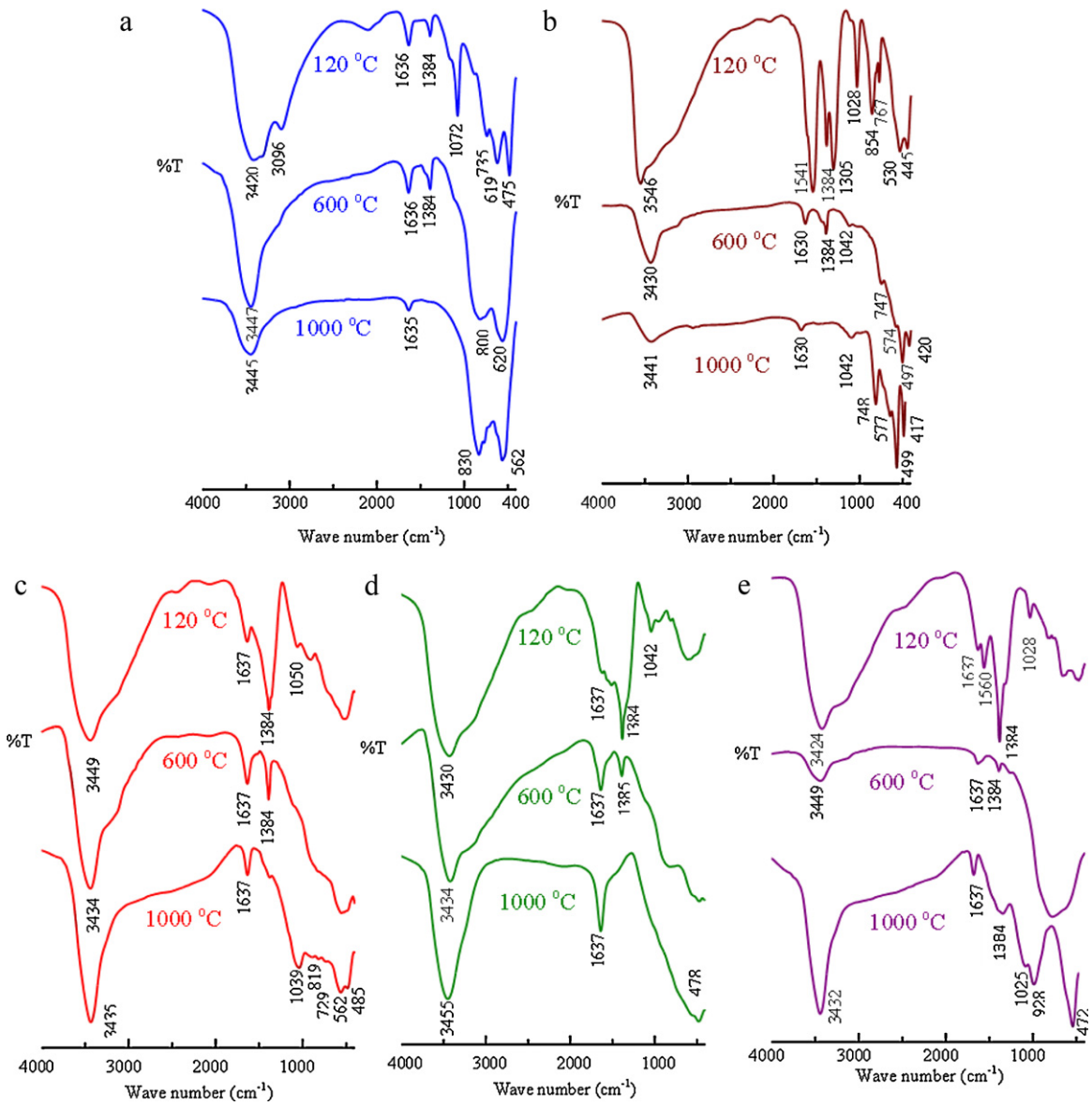

Fig. 6. FT-IR spectrum of mixed Al_2O_3–ZrO_2 composites with different compositions dried/calcined at 120, 600 and 1000 °C: (a) $Al_{100}Zr_0$, (b) Al_0Zr_{100}, (c) $Al_{75}Zr_{25}$, (d) $Al_{50}Zr_{50}$ and (e) $Al_{25}Zr_{75}$.

3.2. Dehydration reaction

Zirconia-based catalysts are known to possess a high selectivity toward the formation of 1-alkenes in the dehydration of secondary alcohols [33–38]. Alumina is an excellent catalyst for the selective dehydration of alcohols [23–25,39–42]. The dehydration studies on secondary alcohols have always been found to be useful in investigating the properties of dehydration catalysts as well as the modes of elimination to yield the various olefins. During the dehydration of alcohol, both intramolecular and intermolecular dehydration may occur. The relative amounts of these pathways depend on the reaction conditions as well as the reactant and catalyst used. The first step of alcohol conversion on metal oxide catalysts is the adsorption of the reactant on the surface. The adsorbed alcohols can be converted through a two-step mechanism involving intermediate carbocation formation (E1), a concerted pathway (E2) or via carbanion formation mechanism (E1cb) [35]. E1 mechanism needs strong acidic catalyst to form carbenium ions by abstraction of OH group. The carbenium ion is rearranged via isomerization followed by abstraction of a β-hydrogen resulting in the thermodynamically controlled alkenes. For E2 mechanism, reaction occurs on dual acid–base sites to eliminate a proton and hydroxyl group which produces the kinetically controlled alkenes, whereas for E1cb mechanism, strong basic sites are required in order to initially remove a β-hydrogen and then eliminate hydroxyl group to produced 1-alkene. The selectivity of secondary and tertiary alcohols dehydration varies depending on which mechanism is acting. Dabbagh et al. [24,43] used both experimental including kinetic and isotopic effect studies and computation analysis to show that dehydration of 2-butanol and 1,2-diphenyl-2-propanol (DPP) over γ-alumina exclusively undergoes E2 elimination.

It is known that the dehydration of alcohols to alkenes over γ-alumina requires temperatures at 100–320 °C, depending on the type of alcohol and catalyst used [44]. Based on the relative thermodynamic stability, any other product formed on the catalyst surface would be expected to immediately dissociate at higher temperatures to give alkene and water [23].

Generally zirconia is known as a basic catalyst. One of the main objectives of this work was to modify the reactivity and selectivity of alumina by adding zirconia. Here, the catalytic activity of

Table 1
Conversion (%) of 2-octanol and DPP over pure and mixed Al_2O_3–ZrO_2 composites at 280 °C.

Catalyst	2-Octanol%	DPP%	(DPP%)/(2-octanol%)
$Al_{100}Zr_0$[a]	44	98	2.23
$Al_{75}Zr_{25}$[a]	73	58	0.79
$Al_{50}Zr_{50}$[a]	25	88	3.52
$Al_{50}Zr_{50}$[b]	1.2	87	72.5
$Al_{25}Zr_{75}$[a]	18	74	4.11
Al_0Zr_{100}[a]	13	98	7.54

[a] Calcined at 600 °C.
[b] Calcined at 1000 °C.

Table 3
Products distribution of dehydration reaction of DPP over pure and mixed Al_2O_3–ZrO_2 composites at 280 °C.

Catalyst	1-Alkene	*E*-2-alkene	*Z*-2-alkene	1-Ene/2-ene	*Z*/*E*
$Al_{100}Zr_0$[a]	50	28.5	21.5	1.00	0.75
$Al_{75}Zr_{25}$[a]	55	11	34	1.22	3.09
$Al_{50}Zr_{50}$[a]	55	33	12	1.22	0.36
$Al_{50}Zr_{50}$[b]	28	70	2	0.39	0.03
$Al_{25}Zr_{75}$[a]	65	24	11	1.86	0.45
Al_0Zr_{100}[a]	54	33	13	1.17	0.35

[a] Calcined at 600 °C.
[b] Calcined at 1000 °C.

Al_2O_3–ZrO_2 composites was evaluated for the dehydration of a mixture of 2-octanol (98 wt.%) and DPP (2 wt.%) using a continuous flow, fixed bed, micro reactor at 280 °C. 2-Octanol (secondary alcohol) and DPP (tertiary alcohol) are very useful models for investigating the catalyst behavior (reactivity vs selectivity). The low concentration of DPP (with higher boiling temperature) prevents saturation over catalyst surface. Results are summarized in Tables 1–3 and compared with those of pure oxides. The conversion of 2-octanol and DPP over pure γ-alumina ($Al_{100}Zr_0$) was 44% and 98% and over pure zirconia (Al_0Zr_{100}) was 13% and 98%, respectively. The high conversion of DPP over both γ-alumina and zirconia must be a result of stronger adsorption of DPP over the surface in comparison to 2-octanol which is due to the higher electron density of phenyl groups in comparison to the alkyl chain. This feature was recently investigated theoretically over γ-alumina by Dabbagh et al. [25]. The reactivity and selectivity of amorphous $Al_{75}Zr_{25}$, $Al_{50}Zr_{50}$, and $Al_{25}Zr_{75}$ composites do not resemble the pure alumina or zirconia. This aspect was previously investigated by XRD and SEM analysis (Section 3.1). Conversion of 73%, 25%, 18% (for 2-octanol) and 58%, 88%, 74% (for DPP) were obtained over $Al_{75}Zr_{25}$, $Al_{50}Zr_{50}$, and $Al_{25}Zr_{75}$ composites, respectively. These results indicated that the $Al_{75}Zr_{25}$ composite is more selective than other composites for the conversion of secondary alcohol (2-octanol). Interestingly, the selectivity of DPP for 1-alkene formation was increased over $Al_{25}Zr_{75}$ catalyst (Scheme 1, Table 3). These finding predicts that 25% content (alumina or zirconia) has pronounce effect on reactivity and selectivity. Reactivity is decreased with increase in % Zr (Table 1). For example, mixed $Al_{75}Zr_{25}$ converted 73% of 2-octanol and 58% of DPP but mixed $Al_{25}Zr_{75}$ converted 18% of 2-octanol and 74% of DPP. Cis/trans ratio is increased by 3-fold depending upon % zirconia. 1-alkene/*E* + *Z*-2-alkenes ratio was increased for 75% zirconia. What causes these changes is the subject of future investigation.

Generally, major products of dehydration of alcohols over alumina and zirconia are alkenes, but isomerization, dehydrogenation, and ether formation as by products are increased with increasing branch of the alcohol hydrocarbon chain or at higher conversion. Therefore, in this study, 2-octanol was used as a solvent and an isomerization preventer. Moreover, the product selectivity (%) of the above pathways depends on the type and preparation method of the catalyst as well as the reaction conditions.

Cis-2-octene is the major products of 2-octanol dehydration over all catalysts (Table 2). The maxima amount of this product (49%) was obtained over the $Al_{75}Zr_{25}$ composite. The minima amount of cis-2-octene (35%) was obtained over $Al_{50}Zr_{50}$ composite. The second major product of 2-octanol conversion was 1-octene. The maxima amount of this product (40%) was observed over $Al_{25}Zr_{75}$ composite and minima amount (26%) was obtained over alumina. The 1-ene/2-ene selectivity for the reaction of 2-octanol over pure ZrO_2 prepared under acidic condition was 0.47 (Table 2). This value for zirconia prepared under basic condition was 4.24 (1-octene 80.5%, trans-2-octene 11.5%, and cis-2-octene 7.5%) which is recently reported by Davis and Chokkaram [37]. Apparently, the basic sites of zirconia are protonated under acidic condition which promote the formation of 2-ene. Stronger basic condition or basic sites are required for the formation of 1-ene. The difference between this work and Davis and Chokkaram results are reasonable and complement to the Ferino et al. [35,38] report which examine the effect of preparation conditions of ZrO_2 catalysts for the dehydration reaction of 4-methylpentane-2-ol. They reported that 2-ene is a major product over ZrO_2 prepared using zirconyl nitrate. The best selectivity for 1-ene was obtained when the precursors were immersed in NaOH. Apparently, the basic sites of zirconia are protonated under acidic condition (this work) which promote the E2 elimination. Stronger basic condition or basic sites are required for E1cb mechanism [35–38].

For DPP dehydration (Scheme 1, Table 3), the major product in all catalysts (>50%) is 1-alkene; and the best selectivity was observed for $Al_{25}Zr_{75}$ composite. For $Al_{75}Zr_{25}$ composite, the second major product was *Z*-2-alkene. These results predict high *Z*/*E* selectivity for $Al_{75}Zr_{25}$ composite.

Conversion percentage of 2-octanol and DPP over amorphous (calcined at 600 °C) and crystalline (calcined at 1000 °C) $Al_{50}Zr_{50}$ composite as a function of reaction time (60 min) is presented in Figs. 7 and 8. The amorphous catalyst converted 25% of 2-octanol to a mixture of cis-2-octene (35%), 1-octene (34%), trans-2-octene (24%), dioctyl ethers (1.3%), isomerization product (3-octenes, 1.3%), dehydrogenation product (2-octanone, 2.7%) and 1.7% unknown side products. The crystalline catalyst converted 1.20% of 2-octanol to a mixture of cis-2-octene (28%), 1-octene (26%), trans-2-octene (17%), 3-octenes (0%), dioctyl ether (0%) and unknown (29%) side products (Tables 1 and 2). These results indi-

Table 2
Products distribution of dehydration reaction of 2-octanol over pure and mixed Al_2O_3–ZrO_2 composites at 280 °C.

Catalyst	1-Octene	Trans-2-octene	Cis-2-octene	3-Octene	2-Octanone	Dioctylether	Others	1-Ene/2-ene	Cis/trans
$Al_{100}Zr_0$[a]	26	23	46	4	0	0.4	0.6	0.38	2.00
$Al_{75}Zr_{25}$[a]	36	14	49	0	0	0.5	0.5	0.57	3.50
$Al_{50}Zr_{50}$[a]	34	24	35	1.3	2.7	1.3	1.7	0.58	1.46
$Al_{50}Zr_{50}$[b]	26	17	28	0	0	0	29	0.58	1.65
$Al_{25}Zr_{75}$[a]	40	11	46	0	0	1.1	2.1	0.70	4.18
Al_0Zr_{100}[a]	28	21	38	5.6	3.7	1.4	2.3	0.47	1.61

[a] Calcined at 600 °C.
[b] Calcined at 1000 °C.

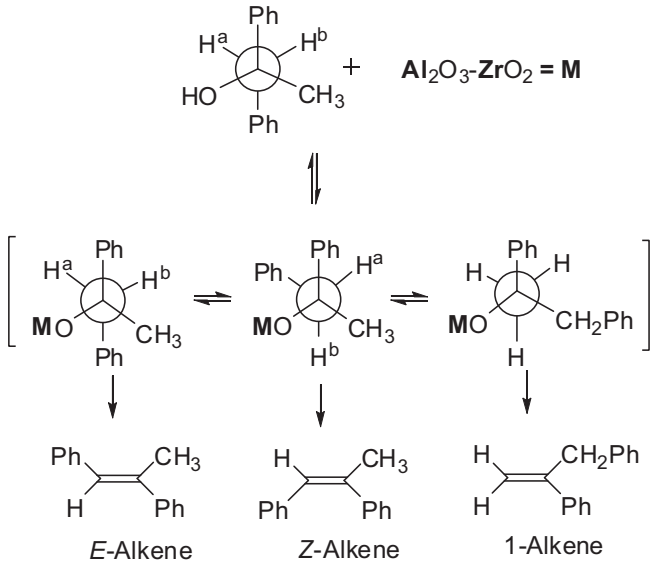

Scheme 1. Schematic representation of DPP dehydration reaction.

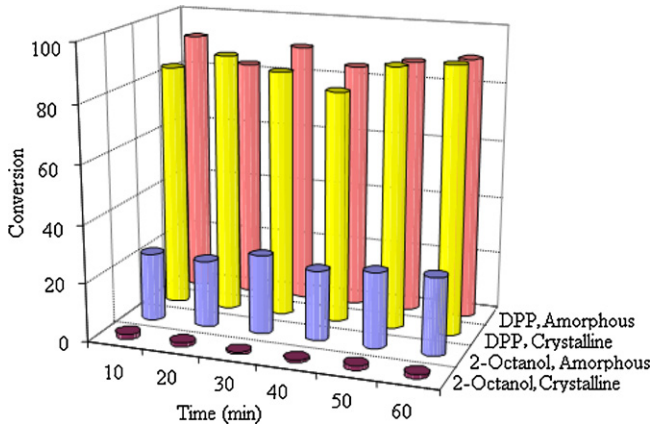

Fig. 7. % Conversion of 2-octanol (● crystalline; ● amorphous) and DPP (● crystalline; ● amorphous) over $Al_{50}Zr_{50}$ catalysts at 280 °C (reaction temperature).

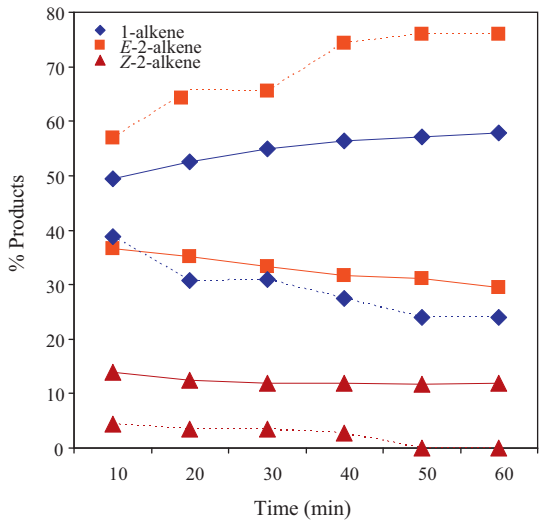

Fig. 8. Products distribution (% *E*-2-alkene (■), *Z*-2-alkene (▲) and 1-alkene (◆)) for the conversion of DPP over amorphous (solid line, —) and crystalline (dotted line, . . .) $Al_{50}Zr_{50}$ catalysts.

cated moderate activity for 2-octanol conversion over amorphous mixed oxide catalyst with interesting product selectivity (equal distribution of cis-2-octene and 1-octene) and 7% side products. Conversion of 2-octanol over crystalline phase was very low producing similar distribution of octenes as amorphous catalyst and 29% side products under the same conditions. The conversion of 2-octanol and DPP over pure γ-alumina which was prepared at 600 °C was 44% and 98% and over pure zirconia (mixture of t- and m-phases) was 13% and 98%, respectively. The product selectivity for the reaction of 2-octanol over pure γ-alumina was 1-alkene (26%), trans-2-octene (23%), cis-2-octene (46%), 3-octenes (4%), dioctyl ethers (0.4%), 2-octanone (0%) and side products (0.6%) and for the reaction of 2-octanol over ZrO_2 was 1-octene (28%), trans-2-octene (21%), cis-2-octene (38%), 3-octenes (5.6%), dioctyl ethers (1.4%), 2-octanone (3.7%) and side products (2.3%).

DPP was converted (88%) over amorphous $Al_{50}Zr_{50}$ catalyst to a mixture of 2-alkene (33% *E*-alkene and 12% *Z*-alkene) and 1-alkene (55%). The crystalline catalyst converted 87% of DPP to 1-alkene (28%), *E*-2-alkene (70%) and *Z*-2-alkene (2%). The conversion of DPP over both catalysts was very high producing mostly 1-alkene over amorphous catalyst and *E*-alkene (which increased at the longer time on stream) over crystalline form (Figs. 7 and 8). The *Z*-2-alkene (%) approached zero at the final times on stream. The product distribution (%) of the reaction of DPP was 1-alkene (54%), *E*-2-alkene (33%) and *Z*-2-alkene (13%) over pure ZrO_2. This selectivity for the DPP conversion over pure γ-alumina was 1-alkene (50%), *E*-2-alkene (28.5%) and *Z*-2-alkene (21.5%), Table 3.

Pure ZrO_2 (mixture of m and t-ZrO_2 phases) converted 13% 2-octanol and 98% DPP, while crystalline 50:50 mixed oxide (mixture of t-ZrO_2 and α-alumina) converted 1.2% 2-octanol and 87% DPP. α-Al_2O_3 is an inactive catalytic toward the dehydration of alcohols. This indicates that zirconia (of the mixed oxide prepared at 1000 °C) is active catalyst for the dehydration of alcohols. The low reactivity of 2-octanol over the crystalline $Al_{50}Zr_{50}$ catalyst is consistent with low surface area (there are limited active sites, pores and crevices to undergo concerted elimination to kinetic controlled products). The small amount of kinetically controlled octenes was produced over this surface. Adsorption and isomerization of these alkenes over the surface also was ruled out. At very low conversion of 2-octanol and relatively low temperature, the rate of 2-octanol adsorption over the surface is much faster than the adsorption of alkenes. Generally, isomerization of alkene over the catalyst surface produces the thermodynamically controlled products which were not observed in this work. In the case of 2-octanol conversion over the crystalline catalyst, both E1 and E2 mechanisms are competing. The E1 mechanism is responsible for the formation of the large amount of secondary products (29%).

The high conversion and unusual product selectivity of DPP over both amorphous and crystalline $Al_{50}Zr_{50}$ catalyst were unpredictable. The high reactivity of DPP over both catalysts must be a result of stronger adsorption of DPP than 2-octanol over the surface which is due to the higher electron density of phenyl groups in comparison to the alkyl chain (minimum surface is required for high conversion of DPP). The unusual selectivity must stem from the structural feature of transition state for each isomer on the surface which favors the formation of 1-alkene (55%) over the amorphous catalyst and *E*-2-alkene (70%) over the crystalline form. These two pathways must have the most feasible conformation and geometry in the transition state with the lowest activation energy. The thermodynamically controlled mixture of alkenes was expected to form over the low surface area catalyst. The ZrO_2 tetragonal phase favors the formation of 1-alkene; and α-Al_2O_3 is an inactive catalytic toward the dehydration of alcohols. This indicates that in the crystalline mixed Al_2O_3/ZrO_2, alumina is apparently poisoned by the catalytic activity of tetragonal zirconia. In other words, doping

of t-ZrO_2 with aluminum atoms generates a catalyst with specific activity and selectivity.

4. Conclusions

Mixed Al_2O_3–ZrO_2 composite with different compositions were prepared by sol–gel method and characterized by XRD, SEM, TGA and FT-IR. Chemically mixed oxide composites calcined at 600 °C are amorphous with no distinct XRD pattern. At 1000 °C the amorphous phase of mixed oxide was transformed to a crystalline phase which consists of t-ZrO_2 and trace of α-Al_2O_3. This feature was observed by TGA and XRD pattern of $Al_{50}Zr_{50}$. Mechanically mixed $Al_{50}Zr_{50}$ composite have XRD pattern similar to those of pure γ-alumina and t, m-zirconia. The specific BET surface area for the $Al_{50}Zr_{50}$ after calcination at 600 and 1000 °C was 104.2 and 0.3 m^2/g, respectively. The NH_3-TPD data complements the BET finding.

Evaluation of catalytic activity and selectivity for dehydration of mixture of 2-octanol and DPP was investigated. Reactivity of 2-octanol was decreased by increasing the zirconium content. This trend was not observed for DPP dehydration. Selectivity for the formation of 1-octene and cis-2-octene was increased for $Al_{25}Zr_{75}$ composite. Octenes isomerization and dehydrogenation was observed only for the $Al_{50}Zr_{50}$ composite and pure zirconia. Minimum ether was formed for the reaction of 2-octanol over $Al_{75}Zr_{25}$ composite. The formation of 1-alkene was increased at the expense of *Z*-2-alkene for the dehydration of DPP over $Al_{25}Zr_{75}$ composite.

The amorphous and crystalline $Al_{50}Zr_{50}$ catalysts showed moderate and very low reactivity for the conversion of 2-octanol respectively, and high conversion for DPP. The crystalline form selectively dehydrated the tertiary alcohol (DPP) in the presence of secondary alcohol (2-octanol) producing *E*-alkene. The amorphous mixed oxide produced the least stable kinetically controlled 1-alkene. This feature of new crystalline Al_2O_3-ZrO_2 (50 wt.%) composite has not been reported elsewhere up to this date.

Acknowledgements

We would like to thank Isfahan University of Technology (IUT) research council for the financial support (Grant # 87/500/9143). We also thank Dr. K. Ghani for his helpful assistant.

Appendix A. Supplementary data

Supplementary data associated with this article can be found, in the online version, at doi:10.1016/j.apcata.2011.07.024.

References

[1] J.S. Valente, X. Bokhimi, F. Hernandez, Langmuir 19 (2003) 3583–3588.
[2] D. Susnik, J. Holc, M. Hrovat, S. Zupancic, J. Mater. Sci. Lett. 16 (1997) 1118–1120.
[3] Q.H. Zhang, Y.Q. Feng, S.L. Da, Anal. Sci. 15 (1999) 767–772.
[4] M. Sugiura, Catal. Surv. Asia 7 (2003) 77–87.
[5] M.Y. He, J.G. Ekerdt, J. Catal. 87 (1984) 238–254.
[6] M.D. Rhodes, K.A. Pokrovski, A.T. Bell, J. Catal. 233 (2005) 210–220.
[7] M. Yoshimura, Ceram. Bull. 67 (1988) 1950–1955.
[8] E.V. Stefanovich, A.L. Shluger, C.R.A. Catlow, Phys. Rev. B 49 (1994) 11560–11571.
[9] G. Stapper, M. Bernasconi, N. Nicoloso, M. Parrinello, Phys. Rev. B 59 (1999) 797–810.
[10] J.H. Bitter, K. Seshan, J.A. Lercher, J. Catal. 183 (1999) 336–343.
[11] H.G. Scott, J. Mater. Sci. 10 (1975) 1527–1535.
[12] R.T. Yang, Adsorbents: Fundamentals and Applications, John Wiley & Sons Inc., 2003, pp. 146–150.
[13] D. Sarkar, D. Mohapatra, S. Ray, S. Bhattacharyya, S. Adak, N. Mitra, Ceram. Int. 33 (2007) 1275–1282.
[14] M. Zawadzki, D. Hreniak, J. Wrzyszcz, W. Mista, H. Grabowska, O.L. Malta, W. Strezka, Chem. Phys. 291 (2003) 275–285.
[15] M. Kagawa, M. Kikuchi, Y. Syono, T. Nagae, J. Am. Ceram. Soc. 66 (1983) 751–754.
[16] G. Kalonji, J. McKittrick, L.W. Hobbs, in: N. Claussen, M. Ruhle, A.H. Heuer (Eds.), Advances in Ceramics, vol. 12, American Ceramic Society, USA, 1984, pp. 816–825.
[17] V. Jayaram, T. Whitney, C.G. Levi, R. Mehrabian, Mater. Sci. Eng. A 124 (1990) 65–81.
[18] J. McKittrick, G. Kalonji, T. Ando, J. Non-Cryst. Sol. 94 (1987) 163–171.
[19] S. Soisuwan, J. Panpranot, D.L. Trimm, P. Praserthdam, Appl. Catal. A: Gen. 303 (2006) 268–272.
[20] J.K. Han, F. Saito, B.T. Lee, Mater. Lett. 58 (2004) 2181–2185.
[21] B.T. Lee, J.K. Han, F. Saito, Mater. Lett. 59 (2005) 355–360.
[22] A. Beitollahi, H. Hosseini-Bay, H. Sarpoolaki, J. Mater. Sci. Mater. Electron. 21 (2010) 130–136.
[23] H.A. Dabbagh, J. Mohammad Salehi, J. Org. Chem. 63 (1998) 7619–7627.
[24] H.A. Dabbagh, M.S. Yalfani, B.H. Davis, J. Mol. Catal. A: Chem. 238 (2005) 72–77.
[25] H.A. Dabbagh, K. Taban, M. Zamani, J. Mol. Catal. A: Chem. 326 (2010) 55–68.
[26] P. Souza Santos, H. Souza Santos, S.P. Toledo, Mater. Res. 3 (2000) 104–114.
[27] K. Jiratova, L. Beranek, Appl. Catal. 2 (1982) 125–138.
[28] H.J.M. Bosman, E.C. Kruissink, J. von der Spoel, F. von den Brink, J. Catal. 148 (1994) 660–672.
[29] M.M. Amini, M. Mirzaee, J. Sol-Gel. Sci. Technol. 36 (2005) 19–23.
[30] L. Le Bihan, F. Dumeignil, E. Payen, J. Grimblot, J. Sol-Gel. Sci. Technol. 24 (2002) 113–120.
[31] D. Sarkar, D. Mohapatra, S. Ray, S. Bhattacharyya, S. Adak, N. Mitra, J. Mater. Sci. 42 (2007) 1847–1855.
[32] S. Roy, J. Sol-Gel. Sci. Technol. 44 (2007) 227–233.
[33] M. Araki, K. Takahashi, T. Hibi, Sumitomo Chemical Co., Eur. Pat. Appl. (1985) 0150832.
[34] M. Araki, T. Hibi, Sumitomo Chemical Co., Eur. Pat. Appl. (1986) 0222356.
[35] I. Ferino, M.F. Casula, A. Corrias, M.G. Cutrufello, R. Monaci, G. Paschina, Phys. Chem. Chem. Phys. 2 (2000) 1847–1854.
[36] K. Tanabe, T. Yamaguchi, Catal. Today 20 (1994) 185–198.
[37] S. Chokkaram, B.H. Davis, J. Mol. Catal. A: Chem. 118 (1997) 89–99.
[38] I. Ferino, A. Auroux, P. Artizzu, J. Chem. Soc. Faraday Trans. 91 (1995) 3263–3267.
[39] B. Shi, H.A. Dabbagh, B.H. Davis, J. Mol. Catal. A: Chem. 141 (1999) 257–262.
[40] H.A. Dabbagh, C.G. Hughes, B.H. Davis, J. Catal. 133 (1992) 445–460.
[41] H. Knozinger, H. Buhl, K. Kochloefl, J. Catal. 24 (1972) 57–68.
[42] V. Macho, M. Kralik, E. Jurecekova, J. Hudec, L. Jurecek, Appl. Catal. A: Gen. 214 (2001) 251–257.
[43] H.A. Dabbagh, M. Zamani, B.H. Davis, J. Mol. Catal. A: Chem. 333 (2010) 54–68.
[44] M.L.G. Franco, S.R. Andrade, R.G. Alamilla, G.S. Robles, J.M.D. Esquivel, Catal. Today 65 (2001) 137–141.